ELSEVIER

Journal of Computational and Applied Mathematics 63 (1995) 179–199

JOURNAL OF COMPUTATIONAL AND APPLIED MATHEMATICS

Combined finite element–finite volume solution of compressible flow[1]

Miloslav Feistauer*, Jiří Felcman, Mária Lukáčová-Medvid'ová

Faculty of Mathematics and Physics, Charles University, Malostranské nám. 25, 118 00 Prague 1, Czech Republic

Received 31 October 1994; revised 5 April 1995

Abstract

The paper is concerned with numerical modelling of inviscid as well as viscous gas flow. The method is based on upwind flux vector splitting finite volume schemes on various types of unstructured grids. In the case of viscous flow we apply a combined method using the finite volume scheme for the discretization of inviscid first order terms of the system and the finite element approximation of viscous dissipative terms. Special attention is paid to higher order schemes and suitable adaptive strategy for a precise resolution of shock waves. Moreover, we summarize the convergence results obtained for a model nonlinear scalar conservation law equation with a diffusion term. Some computational results are presented. In this paper only two-dimensional flow is treated, but the extension to the three-dimensional case is possible.

Keywords: Compressible flow; Euler equations; Navier–Stokes equations; Finite volume method; Upwind flux vector splitting schemes of Godunov type; Adaptive refinement; Shock indicator; MUSCL higher order schemes; Finite element method

1. Formulation of the problem

We consider gas flow in a space–time cylinder $Q_T = \Omega \times (0, T)$, where $\Omega \subset \mathbb{R}^2$ is a bounded domain representing the region occupied by the fluid and $T > 0$. By $\bar{\Omega}$ and $\partial\Omega$ we denote the closure and boundary of Ω, respectively.

The complete system of viscous compressible flow consisting of the continuity equation, Navier–Stokes equations and energy equation can be written in the form

$$\frac{\partial w}{\partial t} + \sum_{i=1}^{2} \frac{\partial f_i(w)}{\partial x_i} = \sum_{i=1}^{2} \frac{\partial R_i(w, \nabla w)}{\partial x_i} \quad \text{in } Q_T. \tag{1.1}$$

* Corresponding author.

[1] This research was supported under the Grant No. 201/93/2177 of the Czech Grant Agency.

SSDI 0377-0427(95)00051-8

Here

$$
\begin{aligned}
&w = (w_1, w_2, w_3, w_4)^{\mathrm{T}} = (\rho, \rho v_1, \rho v_2, e)^{\mathrm{T}},\\
&w = w(x,t), \quad x \in \Omega,\ t \in (0,T),\\
&f_i(w) = (\rho v_i, \rho v_i v_1 + \delta_{i1} p, \rho v_i v_2 + \delta_{i2} p, (e+p)v_i)^{\mathrm{T}},\\
&R_i(w, \nabla w) = (0, \tau_{i1}, \tau_{i2}, \tau_{i1} v_1 + \tau_{i2} v_2 + k\partial\theta/\partial x_i)^{\mathrm{T}},\\
&\tau_{ij} = \lambda \operatorname{div} \boldsymbol{v} \delta_{ij} + \mu\left(\frac{\partial v_i}{\partial x_j} + \frac{\partial v_j}{\partial x_i}\right), \quad i,j = 1,2.
\end{aligned}
\tag{1.2}
$$

From thermodynamics we have

$$
p = (\gamma - 1)(e - \tfrac{1}{2}\rho|\boldsymbol{v}|^2), \quad e = \rho(c_v\theta + \tfrac{1}{2}|\boldsymbol{v}|^2). \tag{1.3}
$$

We use the standard notation: t—time, x_1, x_2—Cartesian coordinates in $\mathbb{R}^2$, ρ—density, $\boldsymbol{v} = (v_1, v_2)$—velocity vector with components v_i in the directions x_i, $i = 1,2$, p—pressure, θ—absolute temperature, e—total energy, τ_{ij}—components of the viscous part of the stress tensor, δ_{ij}—Kronecker delta, $\gamma > 1$—Poisson adiabatic constant, c_v—specific heat at constant volume, k—heat conductivity, λ, μ—viscosity coefficients. We assume that c_v, k, μ are positive constants and $\lambda = -\frac{2}{3}\mu$. We neglect outer volume force. The functions f_i are called inviscid (Euler) fluxes and are defined in the set $D = \{(w_1, \dots, w_4) \in \mathbb{R}^4;\ w_1 > 0\}$. The viscous terms R_i are obviously defined in $D \times \mathbb{R}^8$. (Due to physical reasons it is also suitable to require $p > 0$.)

System (1.1), (1.3) is equipped with the initial conditions

$$
w(x,0) = w^0(x), \quad x \in \Omega \tag{1.4}
$$

(which means that at time $t = 0$ we prescribe, e.g., ρ, v_1, v_2 and θ) and boundary conditions: The boundary $\partial\Omega$ is divided into several disjoint parts. By Γ_{I}, Γ_{O} and Γ_{W} we denote inlet, outlet and impermeable walls, respectively, and assume that

$$
\begin{aligned}
&\rho = \rho^*, \qquad v_i = v_i^*, \quad i = 1,2, \qquad \theta = \theta^* \quad \text{on } \Gamma_{\mathrm{I}},\\
&v_i = 0, \quad i = 1,2, \qquad \frac{\partial\theta}{\partial n} = 0 \quad \text{on } \Gamma_{\mathrm{W}},\\
&\sum_{i=1}^{2} \tau_{ij} n_i = 0, \quad j = 1,2, \qquad \frac{\partial\theta}{\partial n} = 0 \quad \text{on } \Gamma_{\mathrm{O}}.
\end{aligned}
\tag{1.5}
$$

Here $\partial/\partial n$ denotes the derivative in the direction of unit outer normal $\boldsymbol{n} = (n_1, n_2)^{\mathrm{T}}$ to $\partial\Omega$; w^0, ρ^*, v_i^* and θ^* are given functions.

In the solution of a cascade flow problem, Ω is one period of the cascade with $\partial\Omega$ formed by the inlet Γ_{I}, outlet Γ_{O}, impermeable profile Γ_{W} and two piecewise linear artificial cuts Γ^- and Γ^+ such that

$$
\Gamma^+ = \{(x_1, x_2 + \tau);\ (x_1, x_2) \in \Gamma^-\}, \tag{1.6}
$$

where $\tau > 0$ is the width of one period of the cascade in the x_2 direction. On $\Gamma^{\pm}$ we consider the periodicity condition

$$w(x_1, x_2 + \tau) = w(x_1, x_2), \quad (x_1, x_2) \in \Gamma^{-}. \tag{1.7}$$

Let us note that nothing is known about the existence and uniqueness of the solution of problem (1.1), (1.3)–(1.5) (and eventually (1.7)). Some solvability results for system (1.1), (1.3) were obtained either for small data or on a very small time interval under simple Dirichlet boundary conditions (for reference, see e.g., [5, Par. 8.10]). Recently, the global solvability of viscous compressible homoentropic flow (when the energy equation is replaced by the relation $p = p(\rho)$) has been proved under the Dirichlet boundary conditions on $\partial\Omega$ (see [15]).

We do not take care of the lack of theoretical results and deal with the numerical solution of the above problem. Since the viscosity μ and heat conductivity k are small, we treat the diffusion terms on the right-hand side of (1.1) as a perturbation of the inviscid Euler system and conclude that a good method for the solution of viscous flow should be based on a sufficiently robust scheme for inviscid flow simulation. Therefore, we will split the complete system (1.1) into inviscid and viscous parts:

$$\frac{\partial w}{\partial t} + \sum_{i=1}^{2} \frac{\partial f_i(w)}{\partial x_i} = 0, \tag{1.8}$$

$$\frac{\partial w}{\partial t} = \sum_{i=1}^{2} \frac{\partial R_i(w, \nabla w)}{\partial x_i} \tag{1.9}$$

and discretize them separately. First we will pay attention to the inviscid flow problem.

2. Discretization of the inviscid system (1.8)

2.1. *Properties of system* (1.8)

Let us use the following notation:

$$\mathscr{P}(w, \boldsymbol{n}) = \sum_{i=1}^{2} n_i f_i(w),$$

$$\mathbb{A}_i(w) = \mathrm{d} f_i(w)/\mathrm{d}w, \qquad \mathbb{P}(w, \boldsymbol{n}) = \mathrm{d}\mathscr{P}(w, \boldsymbol{n})/\mathrm{d}w = \sum_{i=1}^{2} n_i \mathbb{A}_i(w), \tag{2.1}$$

$$w \in D, \quad \boldsymbol{n} = (n_1, n_2) \in \mathbb{R}^2.$$

($\mathscr{P}(w, \boldsymbol{n})$ is the *flux* of the quantity w in the direction $\boldsymbol{n}$, $\mathbb{A}_i$ and $\mathbb{P}$ are the Jacobi matrices of the mappings f_i and $\mathscr{P}$.) System (1.8) has the following properties:

(1) It is *hyperbolic*, which means that the matrix $\mathbb{P}(w, \boldsymbol{n})$ has real eigenvalues $\lambda_i = \lambda_i(w, \boldsymbol{n})$, $i = 1, 2, 3, 4$, and is diagonalizable: there exists a nonsingular matrix $\mathbb{T} = \mathbb{T}(w, \boldsymbol{n})$ such that

$$\mathbb{P} = \mathbb{T}\mathbb{D}\mathbb{T}^{-1}, \qquad \mathbb{D} = \mathrm{diag}(\lambda_1, \ldots, \lambda_4)$$

($\mathbb{D}$ = diagonal matrix with $\lambda_1, \dots, \lambda_4$ on its diagonal).

(2) System (1.8) is *rotationally invariant*: Denoting

$$\mathbb{Q} = \mathbb{Q}(\boldsymbol{n}) = \begin{pmatrix} 1 & 0 & 0 & 0 \\ 0 & n_1 & n_2 & 0 \\ 0 & -n_2 & n_1 & 0 \\ 0 & 0 & 0 & 1 \end{pmatrix}, \qquad \boldsymbol{n} = (n_1, n_2), \qquad |\boldsymbol{n}| = 1, \tag{2.2}$$

we have

$$\mathscr{P}(w, \boldsymbol{n}) = \mathbb{Q}^{-1} f_1(\mathbb{Q}w), \qquad \mathbb{P}(w, \boldsymbol{n}) = \mathbb{Q}^{-1} \mathbb{A}_1(\mathbb{Q}w)\mathbb{Q}. \tag{2.3}$$

Let us note that the transformation of the Cartesian coordinates of the form

$$\begin{pmatrix} \tilde{x}_1 \\ \tilde{x}_2 \end{pmatrix} = \begin{pmatrix} n_1 & n_2 \\ -n_2 & n_1 \end{pmatrix} \begin{pmatrix} x_1 \\ x_2 \end{pmatrix} + \tilde{\sigma}, \tag{2.4}$$

where $\boldsymbol{n} = (n_1, n_2)$ is a unit vector and $\tilde{\sigma} \in \mathbb{R}^2$, yields a new state vector

$$q = \mathbb{Q}w = (\rho, \rho\tilde{u}, \rho\tilde{v}, e)^{\mathrm{T}}, \qquad \tilde{u} = v_1 n_1 + v_2 n_2, \qquad \tilde{v} = -v_1 n_2 + v_2 n_1, \tag{2.5}$$

satisfying the Euler system

$$\frac{\partial q}{\partial t} + \sum_{i=1}^{2} \frac{\partial f_i(q)}{\partial \tilde{x}_i} = 0. \tag{2.6}$$

(3) The fluxes f_i and $\mathscr{P}$ are *homogeneous* functions of order 1, which implies that

$$f_i(w) = \mathbb{A}_i(w)w, \qquad \mathscr{P}(w, \boldsymbol{n}) = \mathbb{P}(w, \boldsymbol{n})w \tag{2.7}$$

(cf. [5, Par. 7.2.114, 7.3.26]).

Concerning the theory and basic numerical methods for nonlinear hyperbolic systems we refer the reader to an excellent monograph [11]. See also [5, Chap. 7].

2.2. Finite volume method

The above properties allow us to construct efficient numerical schemes for the solution of inviscid flow. We will carry out the discretization of system (1.8) with the use of the finite volume method (FVM) which is now very popular because of its flexibility and applicability and because it reflects well some important characteristic features of compressible flow. We proceed in the following way:

Every component of $\partial\Omega$ is approximated by a piecewise linear curve so that the domain Ω can be replaced by a polygonal domain Ω_h with

$$\partial\Omega_h = \Gamma_{1h} \cup \Gamma_{0h} \cup \Gamma_{wh} \cup \Gamma^- \cup \Gamma^+. \tag{2.8}$$

Here Γ_{1h}, Γ_{Oh}, Γ_{Wh} are parts of $\partial\Omega_h$ approximating Γ_1, Γ_O, Γ_W. We assume that the corners of $\partial\Omega_h$ are elements of $\partial\Omega$. By $\mathscr{D}_h = \{D_i\}_{i\in J}$ we denote a partition of $\bar{\Omega}_h$ into a finite number of closed polygons so that their interiors are mutually disjoint and

$$\bar{\Omega}_h = \bigcup_{i\in J} D_i. \tag{2.9}$$

(J is a suitable index set of nonnegative integers.)

The so-called *finite volumes* D_i are chosen as *triangles, quadrilaterals* or *dual finite volumes* over a triangular mesh $\mathscr{T}_h = \{T_i\}_{i\in I}$ = a triangulation of Ω_h with usual properties used in the finite element method. (See, e.g., [3].) In the latter case, denoting by $\sigma_h = \{P_j\}_{j\in J}$ the set of all vertices of all triangles $T \in \mathscr{T}_h$, we associate each $P_i \in \sigma_h$ with a dual finite volume D_i constructed in the following way: Join the centre of gravity of every triangle $T \in \mathscr{T}_h$, containing the vertex P_i, with the centre of every side of T containing P_i. If $P_i \in \sigma_h \cap \partial\Omega_h$, then we complete the obtained contour by the straight segments joining P_i with the centres of boundary sides that contain P_i. In this way we get the boundary ∂D_i of the finite volume D_i. (See Fig. 1.) Dual finite volume meshes were successfully used in a number of works. See, e.g., [1, 10].

If for two different finite volumes D_i and D_j their boundaries contain a common straight segment, we call them *neighbours*. Then we write

$$\Gamma_{ij} = \bigcup_{\alpha=1}^{\beta_{ij}} \Gamma_{ij}^{\alpha} = \partial D_i \cap \partial D_j = \Gamma_{ji}, \qquad \Gamma_{ij}^{\alpha} = \Gamma_{ji}^{\alpha}, \tag{2.10}$$

where Γ_{ij}^{α} are straight segments. (If $\mathscr{D}_h$ is a triangular or rectangular grid with usual properties from the finite element method, cf. [3], then $\beta_{ij} = 1$.) As follows from above, for a dual finite volume mesh over a triangular grid we have $\beta_{ij} = 2$ (for D_i or $D_j \subset \Omega_h$) or $\beta_{ij} = 1$ (for D_i and D_j adjacent to $\partial\Omega_h$.) For $i \in J$, let $s(i) = \{j \in J; D_j \text{ is a neighbour of } D_i\}$. If D_i is adjacent to $\Gamma_{1h} \cup \Gamma_{Oh} \cup \Gamma_{Wh}$, then we denote by $\Gamma_{i,-1}^{\alpha}$, $\alpha = 1, \ldots, \beta_{i,-1}$, the segments that form $\partial D_i \cap \partial\Omega_h$. In this case we set $S(i) = s(i) \cup \{-1\}$, otherwise we put $S(i) = s(i)$.

In the case of flow past a cascade of profiles, when Ω_h is a polygonal approximation of one period of the cascade and a part of $\partial\Omega_h$ is formed by piecewise linear arcs Γ^-, Γ^+ satisfying (1.6), we assume that the mesh $\mathscr{D}_h$ possesses the *periodicity property*: $\emptyset \neq S_i^- = \partial D_i \cap \Gamma^-$ for some $D_i \in \mathscr{D}_h$ if

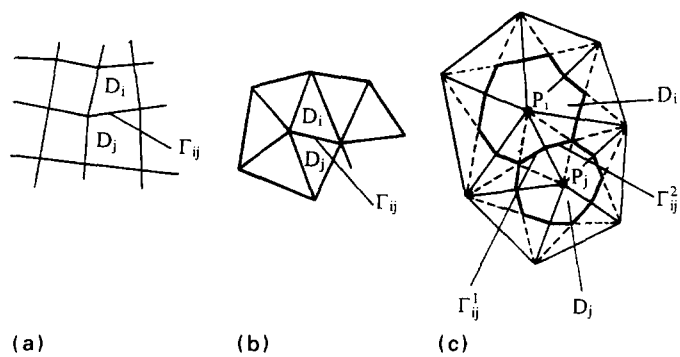

Fig. 1. (a) Quadrilateral mesh; (b) triangular mesh; (c) dual mesh over a triangular grid.

and only if there exists $D_j \in \mathcal{D}_h$ such that

$$S_i^+ = \{(x_1, x_2 + \tau); (x_1, x_2) \in S_i^-\} = \partial D_j \cap \Gamma^+ .$$

In this case we put $\Gamma_{ij} = S_i^-$ and $\Gamma_{ji} = S_i^+$. If the mesh is triangular or quadrilateral, we set $S(i) = s(i) \cup \{j\}, S(j) = s(j) \cup \{i\}$. However, for a *dual mesh over a triangular one* we introduce new finite volumes $D_i' = D_j' = D_i \cup D_j$ and put $S(i) = S(j) = s(i) \cup s(j)$. For the simplicity of the notation we shall omit the superscript $'$ in the sequel.

Obviously, for every $D_i \in \mathcal{D}_h$ we have

$$\partial D_i = \bigcup_{j \in S(i)} \Gamma_{ij} = \bigcup_{j \in S(i)} \bigcup_{\alpha=1}^{\beta_{ij}} \Gamma_{ij}^{\alpha}. \tag{2.11}$$

Furthermore, we introduce the following notation: $|D_i|$ = area of D_i, $\boldsymbol{n}_{ij}^{\alpha} = (n_{1ij}^{\alpha}, n_{2ij}^{\alpha})$ = unit outer normal to ∂D_i on Γ_{ij}^{α}, ℓ_{ij}^{α} = length of Γ_{ij}^{α}, and consider a partition $0 = t_0 < t_1 < \cdots$ of the time interval $(0, T)$ and set $\tau_k = t_{k+1} - t_k$ for $k = 0, 1, \ldots$

The *finite volume (cell centred) discretization* is based on the integration of (1.8) over every set $D_i \times (t_k, t_{k+1})$, the use of Green's theorem, the approximation of the exact solution w averaged at time t_k over grid cells D_i by constant values w_i^k and the approximation of the flux

$$\int_{\Gamma_{ij}^{\alpha}} \sum_{r=1}^{2} f_r(w) n_r \, \mathrm{d}S$$

of the quantity w through the segment Γ_{ij}^{α} in the direction $\boldsymbol{n}_{ij}^{\alpha}$ per second on the time level t_k with the aid of the so-called *numerical flux* $H(w_i^k, w_j^k, \boldsymbol{n}_{ij}^{\alpha})$ calculated from w_i^k, w_j^k and $\boldsymbol{n}_{ij}^{\alpha}$. In this way we obtain the following explicit numerical scheme:

$$w_i^{k+1} = w_i^k - \frac{\tau_k}{|D_i|} \sum_{j \in S(i)} \sum_{\alpha=1}^{\beta_{ij}} H(w_i^k, w_j^k, \boldsymbol{n}_{ij}^{\alpha}) \ell_{ij}^{\alpha}, \quad D_i \in \mathcal{D}_h \text{ (i.e., } i \in J), \quad k = 0, 1, \ldots . \tag{2.12}$$

In case that $j = -1 \in S(i)$ and, thus, $\Gamma_{ij}^{\alpha} \subset \partial\Omega_h$, it is necessary to determine the boundary state on Γ_{ij}^{α}. We will discuss the problem of boundary conditions later.

We require that the *numerical flux H has the following properties*:

(1) H is Lipschitz-continuous on every ball with centre at the origin and radius M with a Lipschitz constant $c(M)$;

(2) H is consistent: $H(w, w, \boldsymbol{n}) = \sum_{r=1}^{2} f_r(w) n_r$ for each $w \in D$ and $\boldsymbol{n} = (n_1, n_2)$, $|\boldsymbol{n}| = 1$;

(3) H is conservative: $H(w, w', \boldsymbol{n}) = -H(w', w, -\boldsymbol{n})$ for all $w, w' \in D$ and $\boldsymbol{n} \in \mathbb{R}^2$, $|\boldsymbol{n}| = 1$.

The properties of system (1.8) mentioned in Section 2.1 allow us to construct Godunov type flux vector splitting schemes. Then the numerical flux H can be expressed in the form

$$H(w_1, w_2, \boldsymbol{n}) = \mathbb{Q}^{-1}(\boldsymbol{n}) f_{\mathrm{R}}(\mathbb{Q}(\boldsymbol{n}) w_1, \mathbb{Q}(\boldsymbol{n}) w_2), \quad w_1, w_2 \in D, \ \boldsymbol{n} \in \mathbb{R}^2, \ |\boldsymbol{n}| = 1, \tag{2.13}$$

where the matrix $\mathbb{Q}(\boldsymbol{n})$ is defined by (2.2) and f_{R} is an *approximate Riemann solver* to the system with one space variable $\tilde{x}_1$ obtained from (2.6) by neglecting the derivative in the direction $\tilde{x}_2$. For details see [5]. In our computations we apply the Vijayasundaram and Osher–Solomon schemes.

In virtue of the hyperbolicity of system (1.8), for any $q \in D$ the matrix $\mathbb{A}_1(q)$ has real eigenvalues $\lambda_i = \lambda_i(q)$, $i = 1, \dots, 4$, and there exists a nonsingular matrix $\mathbb{T} = \mathbb{T}(q)$ such that $\mathbb{A}_1 = \mathbb{T}\mathbb{D}\mathbb{T}^{-1}$, $\mathbb{D} = \operatorname{diag}(\lambda_1, \dots, \lambda_4)$. Then we put

$$\mathbb{A}_1^{\pm} = \mathbb{T}\mathbb{D}^{\pm}\mathbb{T}^{-1}, \qquad \mathbb{D}^{\pm} = \operatorname{diag}(\lambda_1^{\pm}, \dots, \lambda_4^{\pm}), \quad \lambda^{+} = \max(\lambda, 0), \quad \lambda^{-} = \min(\lambda, 0). \tag{2.14}$$

Then the *approximate Riemann solver of the Vijayasundaram method* has the form [5, 21]:

$$f_{\mathrm{V}}(q_1, q_2) = \mathbb{A}_1^{+}\left(\frac{q_1 + q_2}{2}\right) q_1 + \mathbb{A}_1^{-}\left(\frac{q_1 + q_2}{2}\right) q_2 . \tag{2.15}$$

In [5, Par. 7.1.22] it is proved that the eigenvalues $\lambda_i(q)$ of $\mathbb{A}_1(q)$ ($q = (\rho, \rho\tilde{u}, \rho\tilde{v}, e)^{\mathrm{T}}$) and the matrices $\mathbb{T}(q)$ and $\mathbb{T}^{-1}(q)$ have the following form:

$$\lambda_1 = \lambda_2 = \tilde{u}, \quad \lambda_3 = \tilde{u} + c, \quad \lambda_4 = \tilde{u} - c, \quad c = (\gamma p/\rho)^{1/2} = \text{speed of sound}, \tag{2.16}$$

$$\mathbb{T} = \begin{pmatrix} 1 & 0 & \frac{1}{2}c^2 & \frac{1}{2}c^2 \\ \tilde{u} & 0 & (\tilde{u} + c)/2c^2 & (\tilde{u} - c)/2c^2 \\ \tilde{v} & -1 & \tilde{v}/2c^2 & \tilde{v}/2c^2 \\ \frac{1}{2}(\tilde{u}^2 + \tilde{v}^2) & -\tilde{v} & (H + c\tilde{u})/2c^2 & (H - c\tilde{u})/2c^2 \end{pmatrix}, \tag{2.17}$$

$$\mathbb{T}^{-1} = \begin{pmatrix} 1 - (\gamma - 1)(\tilde{u}^2 + \tilde{v}^2)/2c^2 & (\gamma - 1)\tilde{u}c^2 & (\gamma - 1)\tilde{v}/c^2 & -(\gamma - 1)/c^2 \\ \tilde{v} & 0 & -1 & 0 \\ -c\tilde{u} + \frac{1}{2}(\gamma - 1)(\tilde{u}^2 + \tilde{v}^2) & c - (\gamma - 1)\tilde{u} & -(\gamma - 1)\tilde{v} & \gamma - 1 \\ c\tilde{u} + \frac{1}{2}(\gamma - 1)(\tilde{u}^2 + \tilde{v}^2) & -c - (\gamma - 1)\tilde{u} & -(\gamma - 1)\tilde{v} & \gamma - 1 \end{pmatrix}, \tag{2.18}$$

where $H = (e + p)/\rho = c^2/(\gamma - 1) + \frac{1}{2}(\tilde{u}^2 + \tilde{v}^2)$ denotes the enthalpy.

The *Osher–Solomon scheme* [14, 17, 20] was derived with the aid of Riemann invariants to the eigenvectors of the matrix $\mathbb{A}_1(q)$. The resulting approximate Riemann solver can be expressed as a linear combination of values of the vector function $f := f_1$ at uniquely determined and analytically expressed points as can be seen in Table 1.

Table 1
Osher–Solomon Riemann solver $f_{\mathrm{OS}}(q_1, q_2)$

	$\tilde{u}_2 \geqslant -c_2$		$\tilde{u}_2 < -c_2$	
	$\tilde{u}_1 \leqslant c_1$	$\tilde{u}_1 > c_1$	$\tilde{u}_1 \leqslant c_1$	$\tilde{u}_1 > c_1$
$c_A \leqslant \tilde{u}_A$	$f(q_1^{\mathrm{S}})$	$f(q_1)$	$f(q_2) - f(q_2^{\mathrm{S}}) + f(q_1^{\mathrm{S}})$	$f(q_1) - f(q_2^{\mathrm{S}}) + f(q_2)$
$0 < \tilde{u}_A < c_A$	$f(q_A)$	$f(q_1) - f(q_1^{\mathrm{S}}) + f(q_A)$	$f(q_2) - f(q_2^{\mathrm{S}}) + f(q_A)$	$f(q_1) - f(q_2^{\mathrm{S}}) + f(q_2) - f(q_1^{\mathrm{S}}) + f(q_A)$
$-c_B \leqslant \tilde{u}_A \leqslant 0$	$f(q_B)$	$f(q_1) - f(q_1^{\mathrm{S}}) + f(q_B)$	$f(q_2) - f(q_2^{\mathrm{S}}) + f(q_B)$	$f(q_1) - f(q_2^{\mathrm{S}}) + f(q_2) - f(q_1^{\mathrm{S}}) + f(q_B)$
$\tilde{u}_A < -c_B$	$f(q_2^{\mathrm{S}})$	$f(q_1) - f(q_1^{\mathrm{S}}) + f(q_2^{\mathrm{S}})$	$f(q_2)$	$f(q_1) + f(q_2) - f(q_1^{\mathrm{S}})$

The states q_A, q_B, q_1^S, q_2^S are defined in the following way. We set

$$c = (\gamma p/\rho)^{1/2}, \qquad s = p/\rho^\gamma, \qquad \alpha = (s_2/s_1)^{1/2\gamma},$$
$$z_1 = \tfrac{1}{2}(\gamma - 1)\tilde{u}_1 + c_1, \qquad z_2 = \tfrac{1}{2}(\gamma - 1)\tilde{u}_2 - c_2. \tag{2.19}$$

Then

$$c_A = (z_1 - z_2)/(1 + \alpha), \qquad c_B = \alpha c_A, \qquad \rho_A = (c_A/c_1)^{2/(\gamma-1)}\rho_1,$$
$$\rho_B = \rho_A/\alpha^2, \qquad \tilde{u}_A = 2(z_1 - c_A)/(\gamma - 1), \qquad \tilde{u}_B = \tilde{u}_A,$$
$$\tilde{v}_A = \tilde{v}_1, \qquad \tilde{v}_B = \tilde{v}_2, \tag{2.20}$$
$$c_1^S = 2z_1/(\gamma + 1), \qquad \rho_1^S = (c_1^S/c_1)^{2/(\gamma-1)}\rho_1, \qquad \tilde{u}_1^S = c_1^S, \qquad \tilde{v}_1^S = \tilde{v}_1,$$
$$c_2^S = -2z_2/(\gamma + 1), \qquad \rho_2^S = (c_2^S/c_2)^{2/(\gamma-1)}\rho_2, \qquad \tilde{u}_2^S = -c_2^S, \qquad \tilde{v}_2^S = \tilde{v}_2.$$

The mentioned construction is possible under the condition

$$c_1 + c_2 + \tfrac{1}{2}(\gamma - 1)(\tilde{u}_1 - \tilde{u}_2) > \max\{0, \tfrac{1}{2}(\tilde{v}_1 - \tilde{v}_2)\}. \tag{2.21}$$

The Vijayasundaram and Osher–Solomon numerical fluxes satisfy the requirements formulated in Section 2.2.

2.3. *Boundary and initial conditions*

If $\Gamma_{ij}^\alpha \subset \partial\Omega_h$, then special attention must be paid to the determination of boundary conditions, in order to be able to compute the numerical flux $H(w_i^k, w_j^k, \boldsymbol{n}_{ij}^\alpha)$. Namely, it is necessary to specify the *boundary state* $w_j^{k,\alpha} = w_j^k = w_B$. The question of the boundary conditions is rather delicate. We use here such type of boundary conditions which leads to well-posed linearized Riemann initial-boundary value problem (cf. [5, Par. 7.3.43]).

First, let us assume that $\Gamma_{ij}^\alpha \subset \Gamma_{Ih} \cup \Gamma_{Oh} \cup \Gamma_{Wh}$. For the *Vijayasundaram scheme* we prescribe m_p components of the boundary state w_j^k and extrapolate m_e components of w_j^k from D_i onto Γ_{ij}^α, where m_p and m_e is the number of negative and positive eigenvalues of the matrix $\mathbb{P}(w_i^k, \boldsymbol{n}_{ij}^\alpha)$ (cf. (2.1)). It is suitable to distinguish several cases [9]:

(1) *Subsonic inlet* ($-\boldsymbol{v}\cdot\boldsymbol{n} < c$ on D_i): We prescribe ρ, v_1, v_2 on Γ_{ij}^α and extrapolate p from D_i to Γ_{ij}^α.

(2) *Supersonic inlet* ($-\boldsymbol{v}\cdot\boldsymbol{n} \geqslant c$ on D_i): We prescribe ρ, v_1, v_2, p on Γ_{ij}^α.

(3) *Supersonic outlet* ($\boldsymbol{v}\cdot\boldsymbol{n} < c$ on D_i): We prescribe p on Γ_{ij}^α and extrapolate ρ, v_1, v_2 from D_i to Γ_{ij}^α.

(4) *Supersonic outlet* ($\boldsymbol{v}\cdot\boldsymbol{n} \geqslant c$ on D_i): We extrapolate ρ, v_1, v_2, p from D_i to Γ_{ij}^α.

(5) *Solid impermeable boundary*: We extrapolate p from D_i to Γ_{ij}^α and (in virtue of the fact that $\boldsymbol{v}\cdot\boldsymbol{n} = 0$ on impermeable wall) we set

$$H(w_i^k, w_j^k, \boldsymbol{n}_{ij}^\alpha) = p_i^k(0, n_{1ij}^\alpha, n_{2ij}^\alpha, 0)^T. \tag{2.22}$$

In the case of the *Osher–Solomon scheme* we use a modified approach worked out in [20] and further developed in [14]. We introduce the transformed boundary state $q_B = \mathbb{Q}(\boldsymbol{n}_{ij}^\alpha)w_B$ and then

define the corresponding approximate Riemann solver $f_{OS}(q_i, q_B) := f_1(q_B)$:

(1) *Subsonic inlet*: We prescribe $\rho_B, \tilde{u}_B, \tilde{v}_B$ and compute p_B from the formulae

$$p_B = \rho_I c_I^2/\gamma, \qquad \rho_I = (c_I^2 \rho_i/\gamma p_i)^{1/(\gamma-1)}\rho_i, \qquad c_I = c_i + \tfrac{1}{2}(\gamma-1)(\tilde{u}_i - \tilde{u}_B). \tag{2.23}$$

(2) *Supersonic inlet*: We prescribe $\rho_B, \tilde{u}_B, \tilde{v}_B, p_B$.

(3) *Subsonic outlet*: We prescribe p_B and use the formulae

$$\rho_B = \rho_i(p_B/p_i)^{1/\gamma}, \qquad \tilde{u}_B = \tilde{u}_i + \frac{2}{\gamma-1}(c_i - \sqrt{\gamma p_B/\rho_B}), \qquad \tilde{v}_B = \tilde{v}_i. \tag{2.24}$$

(4) *Supersonic outlet*: $q_B = q_i$.

(5) *Impermeable wall*:

$$\tilde{u}_B = 0, \qquad c_B = c_i + \tfrac{1}{2}(\gamma-1)\tilde{u}_i, \qquad \rho_B = (c_B^2 \rho_i/\gamma p_i)^{1/(\gamma-1)}\rho_i, \qquad p_B = \rho_B c_B^2/\gamma \tag{2.25}$$

and we have $f_{OS}(q_i, q_B) = (0, p_B, 0, 0)^T$.

Finally, in the case of a cascade flow when we assume the periodicity of the flow field in the direction x_2 with the period τ, taking into account the definition of the set $S(i)$, we can again use formula (2.12).

In the numerical computations we start from the *initial conditions*

$$w_i^0 = \frac{1}{|D_i|}\int_{D_i} w(x,0)\,dx, \quad i \in J. \tag{2.26}$$

2.4. Stability

Since scheme (2.12) is explicit, it is necessary to apply a suitable stability condition. Using linearization and analogy with a scalar problem we derived the stability condition [5, Par. 7.3.116],

$$\frac{\tau_k}{|D_i|} \max_{\substack{j \in s(i) \\ \alpha = 1,\dots,\beta_{ij}}} \left\{ |\partial D_i| \max_{m=1,\dots,4} \{\lambda_m(\mathbb{Q}(\boldsymbol{n}_{ij}^\alpha) w_i^k)\} \right\} \leqslant \mathrm{CFL} \approx 0.85, \quad i \in J, \tag{2.27}$$

applied both to Vijayasundaram and Osher–Solomon scheme.

Often our goal is to obtain a steady state solution of system (1.8) by *time marching process* as $t_k \to \infty$ using the described schemes and applying the stability condition (2.27).

2.5. Improvement of the accuracy

In practical computations we try to achieve sufficiently accurate solutions with precise resolution of shock waves. There are two possibilities how to increase the accuracy of the method:

(1) the use of MUSCL second order approach;

(2) the use of an adaptive refinement of the mesh.

These two approaches can be, of course, combined.

(I) First, let us describe the method that has a higher order accuracy in space and possesses an adequate rate of dissipation to give physically relevant entropy solution. (The improvement of the accuracy in space is motivated by the search of the steady state solution. In the simulation of

transient flow the higher order accuracy in time can be achieved, e.g., with the aid of Runge–Kutta schemes.)

We start from *the case of a dual finite volume mesh* $\mathscr{D}_h$ constructed over a triangular grid $\mathscr{T}_h$. In order to increase the precision of the method, we replace (2.12) by the formula

$$w_i^{k+1} = w_i^k - \frac{\tau_k}{|D_i|} \sum_{j \in S(i)} \sum_{\alpha=1}^{\beta_{ij}} H((\hat{w}_{ij}^{\alpha})^k, (\hat{w}_{ji}^{\alpha})^k, \boldsymbol{n}_{ij}^{\alpha}) \ell_{ij}^{\alpha}, \quad i \in J, \ k = 0, 1, \ldots, \tag{2.28}$$

where $(\hat{w}_{ij}^{\alpha})^k, (\hat{w}_{ji}^{\alpha})^k$ are values of a higher order recovery of the approximate solution with the values w_i^k on $D_i \in \mathscr{D}_h$ and time level $t = t_k$.

Let φ denote some of the physical quantities ρ, v_1, v_2, p and let φ_i^k denote its approximation on $D_i \times \{t_k\}$ calculated from the components of the state vector w_i^k. For the sake of simplicity we will omit the superscript k (and write simply φ_i instead of φ_i^k, etc.). Now we define the piecewise *linear recovery function* φ_h^* to $\{\varphi_i\}_{i \in J}$ so that $\varphi_h^* : \bar{\Omega}_h \to \mathbb{R}$ is continuous on $\bar{\Omega}_h$, $\varphi_h^*|_T$ is linear for each $T \in \mathscr{T}_h$ and $\varphi_h^*(P_i) = \varphi_i$ for each $i \in J$. This allows us to compute the so-called *averaged gradient*:

$$(\mathrm{grad}_h \varphi_h)|_{D_i} = \frac{1}{|D_i|} \sum_T (\mathrm{grad}\, \varphi_h^*)|_T \, |T \cap D_i|, \tag{2.29}$$

where we sum over all triangles $T \in \mathscr{T}_h$ containing the vertex P_i. Let Z_{ij}^{α} be the midpoint of $\Gamma_{ij}^{\alpha} \not\subset \partial\Omega_h$. For such Γ_{ij}^{α} we define the value

$$\tilde{\varphi}_{ij}^{\alpha} = \varphi_i + (\mathrm{grad}_h \varphi_h)|_{D_i} \cdot (Z_{ij}^{\alpha} - P_i). \tag{2.30}$$

However, this recovery suffers from the lack of dissipation, which reflects in spurious oscillations near discontinuities. The improvement is carried out with the aid of a *flux limiter*. According to [18] we use the Barth–Jespersen flux limiter (see [2]):

$$\phi_i = \min_{j \in s(i)} \Big(\min_{\alpha = 1, \ldots, \beta_{ij}} \phi(\Gamma_{ij}^{\alpha}) \Big),$$

$$\phi(\Gamma_{ij}^{\alpha}) = \begin{cases} 1, & \tilde{\varphi}_{ij}^{\alpha} - \varphi_i = 0, \\ \min\left(1, \dfrac{\varphi_i^{\max} - \varphi_i}{\tilde{\varphi}_{ij}^{\alpha} - \varphi_i}\right), & \tilde{\varphi}_{ij}^{\alpha} - \varphi_i > 0, \\ \min\left(1, \dfrac{\varphi_i^{\min} - \varphi_i}{\tilde{\varphi}_{ij}^{\alpha} - \varphi_i}\right), & \tilde{\varphi}_{ij}^{\alpha} - \varphi_i < 0, \end{cases} \tag{2.31}$$

$$\varphi_i^{\max} = \max\Big(\varphi_i, \max_{j \in s(i)} \varphi_j\Big), \qquad \varphi_i^{\min} = \min\Big(\varphi_i, \min_{j \in s(i)} \varphi_j\Big).$$

Finally, the higher order recovery of the quantity φ is defined on $\Gamma_{ij}^{\alpha} \not\subset \partial\Omega_h$ as

$$\hat{\varphi}_{ij}^{\alpha} = \varphi_i + \phi_i (\mathrm{grad}_h \varphi_h)|_{D_i} \cdot (Z_{ij}^{\alpha} - P_i). \tag{2.32}$$

If we carry out the above recovery $(\hat{\varphi}_{ij}^{\alpha})^k = \hat{\varphi}_{ij}^{\alpha}$ for all quantities $\varphi = \rho, v_1, v_2$ and p, we can construct the value $(\hat{w}_{ij}^{\alpha})^k$ of the state vector.

If $\Gamma_{ij}^{\alpha} \subset \partial\Omega_h$ (i.e. $j = -1$), then we compute $(\hat{w}_{i,-1}^{\alpha})^k$ in the same way as above, but $(\hat{w}_{-1,i}^{\alpha})^k$ is defined by boundary conditions as for the original scheme (2.12).

If the *finite volume mesh* $\mathscr{D}_h$ *is triangular*, we apply the Durlofski–Engquist–Osher approach [4] for computing the higher order recovery $(\hat{w}_{ij}^1)^k = (\hat{w}_{ij}^k)$ and $(\hat{w}_{ji}^1)^k = (\hat{w}_{ji}^k)$. (We have $\beta_{ij} = 1$ in this case.) Let $D_i \in \mathscr{D}_h$ be a triangle with its neighbours D_j, D_l, D_m (i.e., $S(i) = \{j, l, m\}$ and no side of D_i is a part of $\partial\Omega_h$). By Q_r we denote the centre of gravity of a triangle $D_r \in \mathscr{D}_h$. By $\{\varphi_i^k\}_{i \in J}$ we denote the approximate values of a quantity φ on $D_i \times \{t_k\}$. Then we construct three *local linear recoveries* $\hat{\varphi}_{h,ilm}$ = the function linear in $\mathbb{R}^2$ with the values $\hat{\varphi}_{h,ilm}(Q_i) = \varphi_i$, $\hat{\varphi}_{h,ilm}(Q_l) = \varphi_l$, $\hat{\varphi}_{h,ilm}(Q_m) = \varphi_m$ and $\hat{\varphi}_{h,ijm}$, $\hat{\varphi}_{h,ijl}$ which are defined analogously. (For the sake of simplicity, the superscript k is again omitted.) Now we proceed according to the following algorithm:

(1) Select as $\hat{\varphi}_{h,i}$ such $\hat{\varphi}_{h,i\alpha\beta}$ ($(\alpha,\beta) = (l,m)$ or $(\alpha,\beta) = (j,m)$ or $(\alpha,\beta) = (j,l)$) for which $|\nabla\hat{\varphi}_{h,i}|$ is maximal.

(2) Denoting by S_{ir} the midpoint of the side Γ_{ir} of D_i ($r = j, l, m$), we check whether

$$\hat{\varphi}_{h,i}(S_{ij}) \in (\varphi_i, \varphi_j), \qquad \hat{\varphi}_{h,i}(S_{il}) \in (\varphi_i, \varphi_l), \qquad \hat{\varphi}_{h,i}(S_{im}) \in (\varphi_i, \varphi_m). \tag{2.33}$$

(3) If (2.33) is not satisfied, then we choose $\hat{\varphi}_{h,i}$ as $\hat{\varphi}_{h,i\alpha\beta}$ for which $|\nabla\hat{\varphi}_{h,i}|$ is the second largest and repeat the test (2.33). If this condition is not satisfied, then we define $\hat{\varphi}_{h,i}$ as $\hat{\varphi}_{h,i\alpha\beta}$ so that

$$|\nabla\hat{\varphi}_{h,i}| \leqslant \{|\nabla\hat{\varphi}_{h,ilm}|, |\nabla\hat{\varphi}_{h,ijm}|, |\nabla\hat{\varphi}_{h,ijl}|\}. \tag{2.34}$$

(4) We put $\hat{\varphi}_{ir} = \hat{\varphi}_{h,i}(S_{ir})$, $r = j, l, m$. From the values of $\hat{\varphi}_{ir}$ corresponding to the quantities $\varphi := w_1, w_2, w_3, w_4$ we define the states $\hat{w}_{ir}$, $r = j, l, m$, for the given triangle D_i, $i \in J$. Then we use formula (2.28). For D_i adjacent to $\partial\Omega_h$ we use the original scheme (2.12).

(II) Now let us describe our approach to *mesh refinement*. Because the position and form of shock waves are not a priori known, it is convenient to use *adaptive algorithms* using the information of previously computed approximate solution.

The most important tool in an adaptive method is the choice of a suitable error indicator and, for flows with shocks, also a *shock indicator*. Here we are concerned with an adaptive shock capturing algorithm employing a divided differences approach and indicating admissible shock waves only. We have tested several shock indicators on *triangular meshes* (see [6]). The best results were obtained with the aid of the following shock indicator:

$$g(i) = \max_{j \in s(i)} [-(\rho_i - \rho_j)\boldsymbol{v}_i \cdot \boldsymbol{n}_{ij}]^+ / h_i, \quad i \in J, \tag{2.35}$$

where h_i is the length of the longest side of the triangle $D_i \in \mathscr{D}_h =$ the triangular finite volume grid in Ω_h, and $\boldsymbol{v}_i$ is the velocity vector on D_i. (We omit the superscript k.)

The above shock indicator is applied in the following way:

(1) We calculate the *relative indicator*

$$\eta(i) = g(i) / \max_{j \in J} g(j), \quad i \in J. \tag{2.36}$$

(2) If for some $D_i \in \mathcal{D}_h$ we have $\eta(i) \geq \delta$ = a given tolerance, $\delta \in (0, 1)$, then the "mother" triangle D_i is divided into four equal "daughter" subtriangles.

(3) The resulting partition of Ω_h is modified so that the conforming triangulation of Ω_h is obtained.

(4) Initial approximation on the new mesh is defined by taking the same values on the daughter triangles as on the mother triangle.

The above process is repeated in several steps until the desired accuracy and sharpness of the shock wave is obtained.

The described strategy can be easily modified to dual finite volumes over triangular grids.

3. Discretization of the viscous system

The standard approach discretizes the viscous terms also by the finite volume method as it is carried out, e.g., in [8, 12–14, 22]. However, if the inviscid terms in (1.1) are discretized by dual finite volumes over a triangular grid, then the structure of the viscous part of (1.1) offers us the application of the *finite element method.*

First, we describe the finite element discretization of the purely viscous system (1.9) equipped with initial conditions (1.4) and boundary conditions (1.5). Similarly as above we denote by $\mathcal{T}_h$ a triangulation of the domain Ω_h and by P_i, $i \in J$, the vertices of all triangles $T \in \mathcal{T}_h$. We use conforming piecewise linear finite elements. This means that the components of the state vector are approximated by functions from the finite dimensional space

$$X_h = \{\varphi_h \in C(\bar{\Omega}_h);\ \varphi_h|_T \text{ is linear for each } T \in \mathcal{T}_h\}. \tag{3.1}$$

Further, we set $\boldsymbol{X}_h = [X_h]^4$ and

$$\boldsymbol{V}_h = \{\varphi_h = (\varphi_1, \varphi_2, \varphi_3, \varphi_4) \in \boldsymbol{X}_h,\ \varphi_i = 0 \text{ on the part of } \partial\Omega_h \text{ approximating the part of } \partial\Omega \text{ where } w_i \text{ satisfies the Dirichlet condition}\}, \tag{3.2a}$$

$$\boldsymbol{W}_h = \{w_h \in \boldsymbol{X}_h; \text{ its components satisfy the Dirichlet boundary conditions following from (1.5)}\}. \tag{3.2b}$$

Multiplying (1.9) considered on time level t_k by any $\varphi_h \in \boldsymbol{V}_h$, integrating over Ω_h, using Green's theorem, taking into account the boundary conditions (1.5) and approximating the time derivative by a forward finite difference, we obtain the following *explicit scheme* for the calculation of an approximate solution w_h^{k+1} on the $(k+1)$st time level:

$$w_h^{k+1} \in \boldsymbol{W}_h, \tag{3.3a}$$

$$\int_{\Omega_h} w_h^{k+1}\varphi_h \,\mathrm{d}x = \int_{\Omega_h} w_h^k \varphi_h \,\mathrm{d}x - \tau_k \int_{\Omega_h} \sum_{s=1}^{2} R_s(w_h^k, \nabla w_h^k) \frac{\partial \varphi_h}{\partial x_s} \,\mathrm{d}x \quad \forall \varphi_h \in \boldsymbol{V}_h. \tag{3.3b}$$

Replacing $R_s(w_h^k, \nabla w_h^k)$ by $R_s(w_h^{k+1}, \nabla w_h^{k+1})$, we obtain an *implicit scheme.*

The integrals are approximated by a numerical quadrature, called *mass lumping*, using the vertices of triangles as integration points:

$$\int_T F\,\mathrm{d}x \approx \frac{1}{3}|T| \sum_{i=1}^{3} F(P_T^i) \tag{3.4}$$

for $F \in C(T)$ and a triangle $T = T(P_T^1, P_T^2, P_T^3) \in \mathcal{T}_h$ with vertices $P_T^i \in \sigma_h$, $i = 1,2,3$. Numerical integration in (3.3b) yields the identity

$$(w_h^{k+1}, \varphi_h)_h = (w_h^k, \varphi_h)_h - \tau_k a_h(w_h^k, \varphi_h) \quad \forall \varphi_h \in V_h, \tag{3.5}$$

where

$$(w_h, \varphi_h)_h = \frac{1}{3} \sum_{T \in \mathcal{T}_h} |T| \sum_{i=1}^{3} w_h(P_T^i)\,\varphi_h(P_T^i), \quad w_h, \varphi_h \in X_h \tag{3.6}$$

and

$$\begin{aligned}
&a_h(w_h, \varphi_h) = (a_h^1(w_h, \varphi_h), \dots, a_h^4(w_h, \varphi_h))^{\mathrm{T}},\\
&a_h^1 \equiv 0,\\
&a_h^2(w_h, \varphi_h) = \sum_{T \in \mathcal{T}_h} |T| \left\{ 2\mu \frac{\partial v_{h,1}}{\partial x_1}\bigg|_T \frac{\partial \varphi_{h,2}}{\partial x_1}\bigg|_T + \lambda(\operatorname{div} v_h)|_T \frac{\partial \varphi_{h,2}}{\partial x_1}\bigg|_T \right.\\
&\qquad \left. + \mu\left(\frac{\partial v_{h,2}}{\partial x_1}\bigg|_T + \frac{\partial v_{h,1}}{\partial x_2}\bigg|_T \right) \frac{\partial \varphi_{h,2}}{\partial x_2}\bigg|_T \right\},\\
&a_h^3(w_h, \varphi_h) = \sum_{T \in \mathcal{T}_h} |T| \left\{ \mu\left(\frac{\partial v_{h,2}}{\partial x_1}\bigg|_T + \frac{\partial v_{h,1}}{\partial x_2}\bigg|_T \right) \frac{\partial \varphi_{h,3}}{\partial x_1}\bigg|_T \right.\\
&\qquad \left. + 2\mu \frac{\partial v_{h,2}}{\partial x_2}\bigg|_T \frac{\partial \varphi_{h,3}}{\partial x_2}\bigg|_T + \lambda(\operatorname{div} v_h)|_T \frac{\partial \varphi_{h,3}}{\partial x_2}\bigg|_T \right\},\\
&a_h^4(w_h, \varphi_h) = \sum_{T \in \mathcal{T}_h} \left\{ \frac{1}{3}|T| \left(\tau_{h,11}|_T \sum_{i=1}^{3} v_{h,1}(P_T^i) + \tau_{h,12}|_T \sum_{i=1}^{3} v_{h,2}(P_T^i) \right) \frac{\partial \varphi_{h,4}}{\partial x_1}\bigg|_T \right.\\
&\qquad + \frac{1}{3}|T| \left(\tau_{h,21}|_T \sum_{i=1}^{3} v_{h,1}(P_T^i) + \tau_{h,22}|_T \sum_{i=1}^{3} v_{h,2}(P_T^i) \right) \frac{\partial \varphi_{h,4}}{\partial x_2}\bigg|_T\\
&\qquad \left. + k|T| \sum_{j=1}^{2} \frac{\partial \theta_h}{\partial x_j}\bigg|_T \frac{\partial \varphi_{h,4}}{\partial x_j}\bigg|_T \right\},\\
&\tau_{h,rs}|_T = \frac{1}{2}\left(\frac{\partial v_{h,r}}{\partial x_s} + \frac{\partial v_{h,s}}{\partial x_r} \right)\bigg|_T = \text{const.}
\end{aligned} \tag{3.7}$$

Here $v_{h,s}$ and θ_h represent functions from the space X_h approximating the velocity components and temperature.

It is easy to write down the implicit variant of (3.5).

Finally, we come to the *discretization of the complete viscous system.* We combine the finite volume discretization of the inviscid system (1.8) on the dual finite volume mesh $\mathscr{D}_h$ (see Section 2.1) with the finite element discretization of the purely viscous system (1.9). We can proceed in several ways:

(1) *Inviscid–viscous operator splitting.* We start from the approximation w_i^0, $D_i \in \mathscr{D}_h$, of the initial condition given by (2.26). Let us assume that we have already obtained the values w_i^k, $D_i \in \mathscr{D}_h$, of the approximate solution of the dual mesh $\mathscr{D}_h$ at time t_k. The transition to the next time level is carried out in two *fractional steps*:

(i) Compute

$$w_i^{k+1/2} = w_i^k - \frac{\tau_k}{|D_i|} \sum_{j \in S(i)} \sum_{\alpha=1}^{\beta_{ij}} H(w_i^k, w_j^k, \boldsymbol{n}_{ij}^\alpha) \ell_{ij}^\alpha, \quad D_i \in \mathscr{D}_h,$$

& inviscid boundary conditions from Section 2.3;

(ii) (α) Define $w_h^{k+1/2} \in \boldsymbol{X}_h$ such that $w_h^{k+1/2}(P_i) = w_i^{k+1/2}$, $i \in J$. (3.8)

(β) Compute $w_h^{k+1} \in \boldsymbol{W}_h$ such that

$$(w_h^{k+1}, \varphi_h)_h = (w_h^{k+1/2}, \varphi_h)_h - \tau_k a_h(w_h^{k+1/2}, \varphi_h) \; \forall \varphi_h \in \boldsymbol{V}_h,$$

(γ) Set $w_i^{k+1} = w_h^{k+1}(P_i)$, $i \in J$, $k := k+1$, go to (i).

(3.8, i) is obtained from scheme (2.12). It can be replaced in an obvious way by the higher order scheme (2.28). In (3.8, ii-β), it is possible to consider the implicit variant.

(2) *Direct discretization of the viscous problem.* Let us define the form

$$b_h(w_h, \varphi_h) = \sum_{P_i \in \sigma_h} \varphi_h(P_i) \sum_{j \in S(i)} \sum_{\alpha=1}^{\beta_{ij}} H(w_h(P_i), w_h(P_j), \boldsymbol{n}_{ij}^\alpha) \ell_{ij}^\alpha, \quad w_h, \varphi_h \in \boldsymbol{X}_h. \tag{3.9}$$

It is possible to show that (3.8, i) can be rewritten as

$$(w_h^{k+1/2}, \varphi_h)_h = (w_h^k, \varphi_h)_h - \tau_k b_h(w_h^k, \varphi_h), \quad \varphi_h \in \boldsymbol{V}_h. \tag{3.10}$$

This leads us to the direct discretization of the complete system (1.1) in the fully explicit form

$$w_h^{k+1} \in \boldsymbol{W}_h, \tag{3.11a}$$

$$(w_k^{k+1}, \varphi_h)_h = (w_h^k, \varphi_h)_h - \tau_k [b_h(w_h^k, \varphi_h) + a_h(w_h^k, \varphi_h)], \quad \varphi_h \in \boldsymbol{V}_h, \tag{3.11b}$$

or in the semi-implicit form

$$w_h^{k+1} \in \boldsymbol{W}_h, \tag{3.12a}$$

$$(w_h^{k+1}, \varphi_h)_h = (w_h^k, \varphi_h)_h - \tau_k [b_h(w_h^k, \varphi_h) + a_h(w_h^{k+1}, \varphi_h)], \quad \varphi_h \in \boldsymbol{V}_h. \tag{3.12b}$$

The form b_h can be replaced by its higher order version

$$\hat{b}_h(w_h, \varphi_h) = \sum_{P_i \in \sigma_h} \varphi_h(P_i) \sum_{j \in S(i)} \sum_{\alpha=1}^{\beta_{ij}} H(\hat{w}_{ij}^\alpha, \hat{w}_{ji}^\alpha, \boldsymbol{n}_{ij}^\alpha) \ell_{ij}^\alpha, \quad w_h, \varphi_h \in \boldsymbol{X}_h, \tag{3.13}$$

where $\hat{w}_{ij}^\alpha$ and $\hat{w}_{ji}^\alpha$ represent the values of the higher order recovery defined in the same way as in Section 2.5 with the aid of the values $w_i = w_h(P_i)$, $i \in J$.

The above schemes can be applied only under some stability conditions. In virtue of the explicit discretization of inviscid terms we apply the stability condition (2.27). In the case of explicit discretization of the viscous terms (scheme (3.8, ii) or (3.11)) we consider, moreover, the additional stability condition in the form

$$\frac{3}{4}\frac{h}{\sigma}\frac{\tau_k}{|T|}\max(\mu,k) \leqslant \mathrm{CFL}, \quad T \in \mathscr{T}_h, \tag{3.14}$$

where h is the length of the maximal side in $\mathscr{T}_h$ and $\sigma = \min_{T\in\mathscr{T}_h}\sigma_T$, σ_T = radius of the largest circle inscribed into T.

4. Convergence

The attempts to prove the convergence of numerical methods for the solution of the complete system describing viscous flow have not yet been successful. Therefore, in order to support our computational results obtained by the combined finite volume – finite element method, we confine our convergence analysis to a model scalar nonlinear convection – diffusion conservation law equation

$$\frac{\partial u}{\partial t} + \sum_{i=1}^{2}\frac{\partial f_i(u)}{\partial x_i} = \nu\Delta u \quad \text{in } \Omega, \tag{4.1}$$

equipped with initial and boundary conditions

$$u(x,0) = u^0(x), \quad x \in \Omega, \tag{4.2}$$

$$u|_{\partial\Omega\times(0,T)} = 0. \tag{4.3}$$

We assume that $\nu > 0$ is a constant, $f_i \in C^1(\mathbb{R})$ and consider (4.1)–(4.3) formulated in a *weak sense*: Find $u \in L^2(0,T; H_0^1(\Omega))$ such that

$$\frac{\mathrm{d}}{\mathrm{d}t}\int_\Omega u(\cdot,t)v\,\mathrm{d}x - \int_\Omega \sum_{i=1}^{2} f_i(u(\cdot,t))\frac{\partial v}{\partial x_i}\,\mathrm{d}x + \nu\int_\Omega \nabla u(\cdot,t)\cdot\nabla v\,\mathrm{d}x = 0 \quad \forall v \in H_0^1(\Omega) \tag{4.4}$$

in the sense of distributions over $(0,T)$. Under some assumptions on f_i we find that $u \in C([0,T], (H_0^1(\Omega))^*)$ and, hence, the initial condition (4.2) has sense. By $H_0^1(\Omega)$ we denote the well-known Sobolev space of all functions square integrable over Ω together with their first order distribution derivatives with zero traces on $\partial\Omega$. $L^2(0,T; H_0^1(\Omega))$ denotes the Bochner space of square integrable functions with values in $H_0^1(\Omega)$. $(H_0^1(\Omega))^*$ is the dual of $H_0^1(\Omega)$.

We will formulate two sorts of results for scheme (3.12a), (3.12b). Denoting by $u_h^0, u_h^1, \ldots, u_h^N$ the values of the approximate solution at time instants $t_k = k\tau$, $k = 0,1,\ldots,N$, $\tau = T/N$, we construct the piecewise linear continuous function $u_{h\tau}: [0,T] \to H_0^1(\Omega)$ such that $u_{h\tau}(t_k) = u_h^k$ for $k = 0,\ldots,N$.

(I) Lukáčová-Medvid'ová proved in [16] the convergence of approximate solutions $u_{h\tau}$ obtained by scheme (3.12a), (3.12b) to the unique weak solution of (4.1)–(4.3) under the assumption of "small data".

Theorem 4.1. *Let $f_i(u) = v_i(u)u$, $v_i \in C^1(\mathbb{R})$, there exist constants $c_1, c_2 > 0$ such that*

$$|v_i(u)| \leqslant c_1|u|, \quad \left|\frac{dv_i(u)}{du}\right| \leqslant c_2, \qquad u \in \mathbb{R},\ i = 1, 2, \tag{4.5}$$

$u^0 \in H_0^1(\Omega)$, the numerical flux H has properties (1)–(3) from Section 2.2, u_h^0 is the Ritz projection of u^0, consider a regular system of triangulations $\{\mathcal{T}_h\}_{h\in(0,h_0)}$ and let the stability condition be fulfilled:

$$\text{there exist } C_1, C_2 > 0,\ \alpha \in [0,1) \text{ such that } C_1 \leqslant \frac{\tau}{h^{1+\alpha}} \leqslant C_2. \tag{4.6}$$

Moreover, we assume that $c_1, c_2 \ll 1$, $\|u^0\|_{H^1(\Omega)} \ll 1$. Then

$$\begin{aligned} &u_{h\tau} \to u \quad \text{weakly in } L^2(0,T; H_0^1(\Omega)),\\ &u_{h\tau} \to u \quad \text{strongly in } L^2(Q_T),\\ &\qquad \text{as } h, \tau \to 0, \end{aligned} \tag{4.7}$$

and u is the unique weak solution of problem (4.1)–(4.3).

(II) In [7] we have proved the convergence result without any restriction of f_i, but under additional assumptions on the triangulation $\mathcal{T}_h$ and numerical flux H:

Theorem 4.2. *Let us assume that $f_i \in C^1(\mathbb{R})$, $u^0 \in W^{1,p}(\Omega)$, $p > 2$, $u_h^0 = r_h u^0$ = the Lagrange interpolation of u^0, $\{\mathcal{T}_h\}_{h\in(0,h_0)}$ is a regular system of weakly acute type triangulations (all angles of all $T \in \mathcal{T}_h$ are $\leqslant \frac{1}{2}\pi$), the numerical flux H has properties (1)–(3) from Section 2.2 and is monotone (i.e., $H(u, v, \boldsymbol{n})$ is nonincreasing with respect to v), $|u^0| \leqslant M$ for some M and*

$$\tau c(M)|\partial D_i| \leqslant |D_i|, \quad i \in J,\ h \leqslant \text{const}\ v,\ h, \tau \to 0.$$

Then

$$\begin{aligned} &u_{h\tau} \to u \quad \text{weakly in } L^2(0,T; H_0^1(\Omega)),\\ &u_{h\tau} \to u \quad \text{weak-}* \text{ in } L^\infty(Q_T),\\ &u_{h\tau} \to u \quad \text{strongly in } L^2(Q_T),\\ &\qquad \text{as } h, \tau \to 0, \end{aligned} \tag{4.8}$$

where $u \in L^2(0,T; H_0^1(\Omega)) \cap L^\infty(Q_T)$ is the unique weak solution of (4.1)–(4.3).

5. Computational results

(1) *Flow through the GAMM channel* (10% circular arc in the channel of width 1 m) for air, i.e., $\gamma = 1.4$, and inlet Mach number $M = 0.67$ was solved by the Vijayasundaram higher order scheme applied on the dual mesh over a triangular grid (see Section 2.5(I)). In Fig. 2 the basic grid and dual mesh, respectively, are shown. Our aim was to obtain the steady state solution with the aid of time marching process for $t_k \to \infty$. Fig. 3 shows the history of the convergence

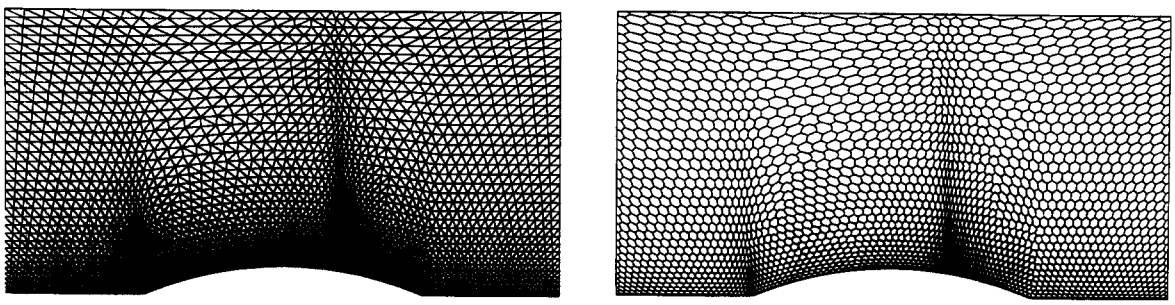

Fig. 2. Triangular mesh in the GAMM channel and the dual mesh.

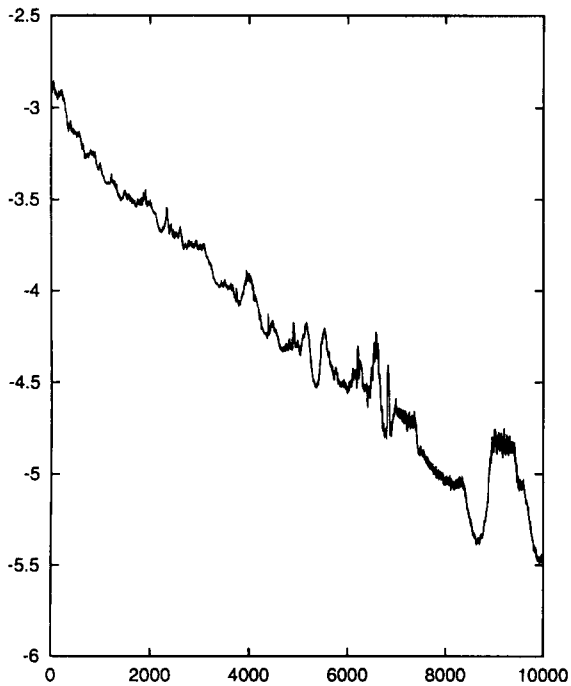

Fig. 3. Convergence history measured in L^1-norm.

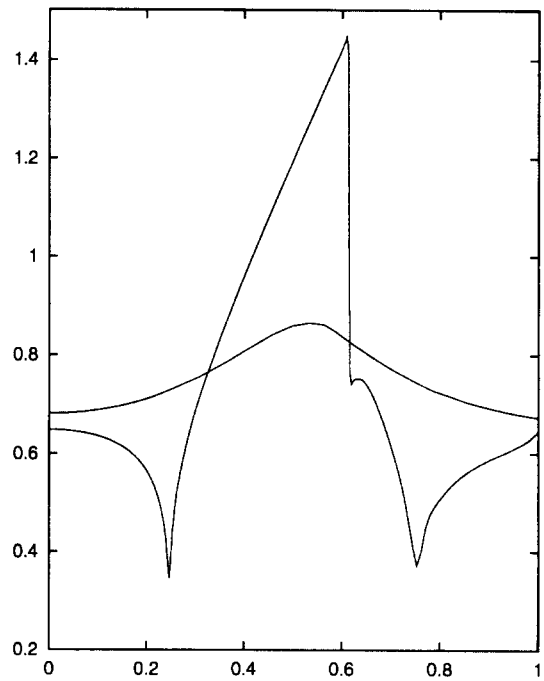

Fig. 4. Mach number distribution on the walls of the channel.

measured in L^1-norm, i.e., the behaviour of the quantity $\log\{\sum_{i\in J}|D_i|\,|(\rho_i^{k+1}-\rho_i^k)/\rho_i^k|\}$, in the dependence on k. Further, in Fig. 4 we see the Mach number distribution on the walls of the channel and Fig. 5 shows Mach number isolines and entropy isolines.

(2) *Inviscid flow past a cascade of profiles* was solved by the Osher–Solomon scheme applied on a triangular mesh with the aid of adaptive technique described in Section 2.5(II) for a turbine cascade for which the wind tunnel measurements were carried out. Fig. 6 shows the adaptively refined mesh in the vicinity of shock waves and Mach number isolines computed with the aid of the

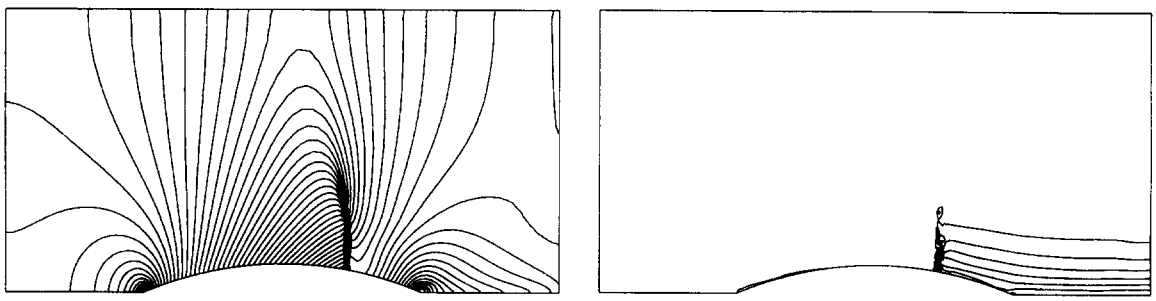

Fig. 5. Mach number isolines and entropy isolines.

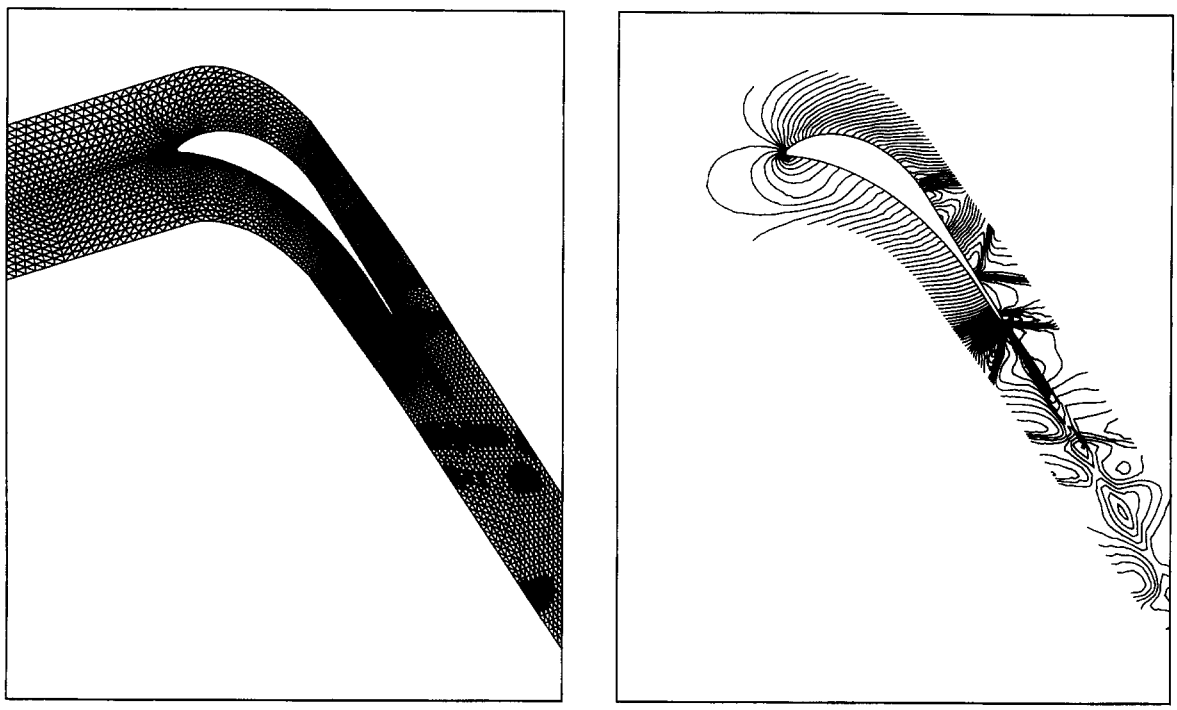

Fig. 6. Mesh and Mach number isolines for inviscid cascade flow.

first order Osher–Solomon scheme. Fig. 7 represents the detail of the Mach number isolines and the comparison with a wind tunnel experiment (the courtesy of the Institute of Thermomechanics of the Czech Academy of Sciences in Prague). The experiment as well as the computation were performed for the following data: angle of attack = 19°18′, inlet Mach number = 0.32, outlet Mach number = 1.18, $\gamma = 1.4$. The coincidence of experimental and computational results is very satisfactory, although the real viscous gas flow is modelled with the aid of the inviscid Euler system. For further details, see [6].

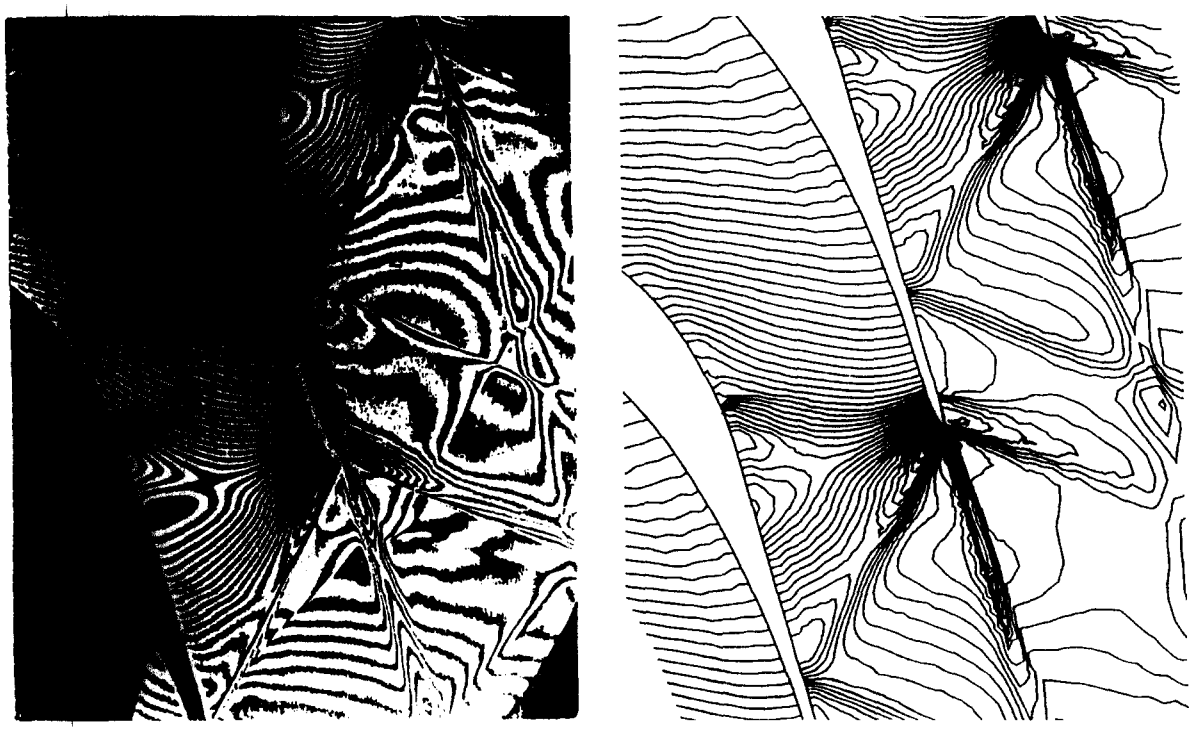

Fig. 7. Detail of Mach number isolines compared with the interferogram of the cascade flow.

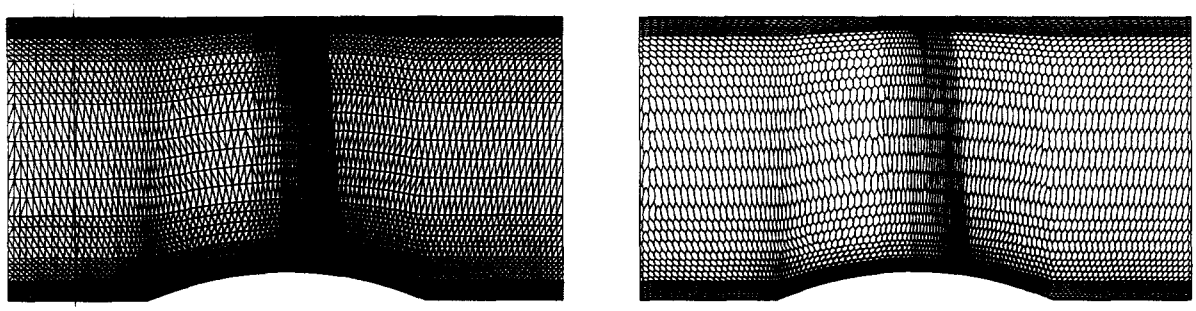

Fig. 8. Triangular mesh and dual mesh for viscous flow.

(3) *Viscous flow through the GAMM channel* was computed for the following data: $\gamma = 1.4$, $\mu = 1.72 \cdot 10^{-5}\,\mathrm{kg\,m^{-1}\,s^{-1}}$, $\lambda = -1.15 \cdot 10^{-5}\,\mathrm{kg\,m^{-1}\,s^{-1}}$, $k = 2.4 \cdot 10^{-2}\,\mathrm{kg\,m\,s^{-3}\,K^{-1}}$, $c_v = 721.428\,\mathrm{J\,kg\,K^{-1}}$ and the inlet Mach number $M = 0.67$.

The solution of viscous flow was carried out by purely explicit combined finite volume – finite element inviscid–viscous operator splitting scheme (3.8, i–ii) using the Vijayasundaram numerical flux for the approximation of inviscid terms. In Fig. 8 we see the triangulation of the channel and the corresponding dual mesh that were used for the realization of the viscous and inviscid part of the scheme, respectively. The length of the time step τ was controlled by the stability conditions (2.27) and (3.14).

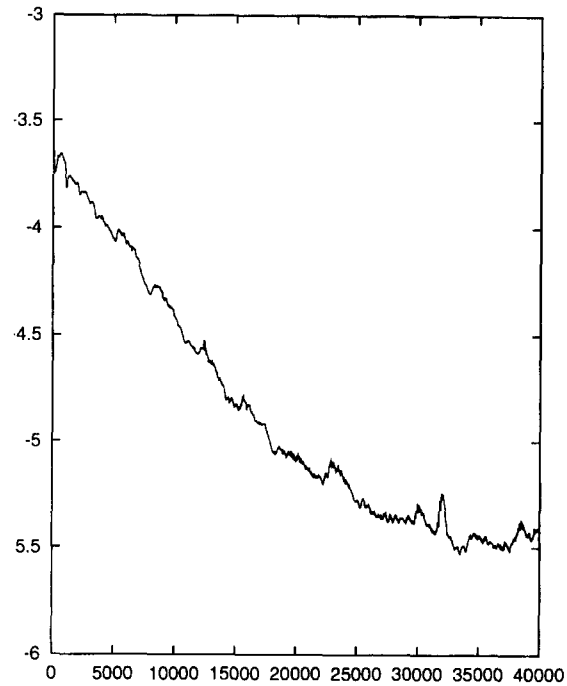

Fig. 9. Convergence history in L^1-norm for the computation of viscous flow.

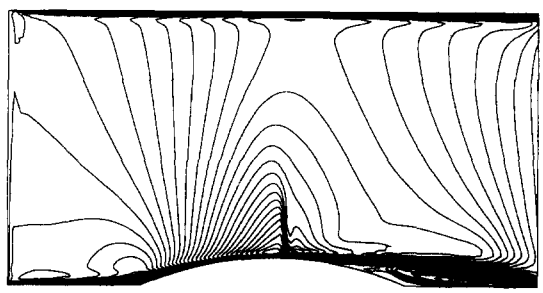

Fig. 10. Mach number isolines of viscous flow.

Fig. 9 shows the convergence history measured in the same way as above in L^1-norm. In Fig. 10 Mach number isolines are drawn. Here we can see boundary layer at the walls, shock wave, wake and the interaction of the shock with boundary layer.

References

[1] P. Arminjou, A. Dervieux, L. Fezoui, H. Steve and B. Stoufflet, Non-oscillatory schemes for multidimensional Euler calculations with unstructured grids, in: J. Ballmann and R. Jeltsch, Eds., *Nonlinear Hyperbolic Equations — Theory, Computation Methods, and Applications*, Notes Numer. Fluid Mech. **24** (Vieweg, Braunschweig, 1989) 1–10.

[2] T.J. Barth and D.C. Jespersen, The design and application of upwind schemes on unstructured meshes, *AIAA Paper* **336**, 1989.
[3] P.G. Ciarlet, *The Finite Element Method for Elliptic Problems* (North-Holland, Amsterdam, 1979).
[4] L.J. Durlofski, B. Enquist and S. Osher, Triangle based adaptive stencils for the solution of hyperbolic conservation laws, *J. Comput. Phys.* **98** (1990) 64–73.
[5] M. Feistauer, *Mathematical Methods in Fluid Dynamics*, Pitman Monographs Surveys Pure Appl. Math. **67** (Longman, Harlow, 1993).
[6] M. Feistauer, J. Felcman and V. Dolejší, Adaptive finite volume method for the numerical solution of the compressible Euler equations, in: S. Wagner, E.H. Hirschel, J. Périaux and R. Piva, Eds., *Computational Fluid Dynamics 94*, Vol. 2, *Proc. 2nd European CFD Conf.* (Wiley, New York, 1994) 894–901.
[7] M. Feistauer, J. Felcman and M. Lukáčová-Medvid'ová, On the convergence of a combined finite volume – finite element method for nonlinear convenction–diffusion problems, Preprint, Faculty of Math. and Physics, Charles University, Prague, 1994.
[8] M. Feistauer and P. Knobloch, Operator splitting method for compressible Euler and Navier–Stokes equations, in: *Proc. Internat. Workshop on Numerical Methods for the Navier–Stokes Equations*, Heidelberg, 1993, Notes Numer. Fluid Mech. **47** (Vieweg, Braunschweig, 1994) 70–78.
[9] J. Felcman, Application d'un schéma de Godounov à des écoulements transsoniques bidimensionnels, in: *Actes de IIèmes Journées Saragosse–Pau de Mathématiques Appliquées* (Université de Pau, 1992) 119–129.
[10] J. Fezoui and B. Stoufflet, A class of implicit schemes for Euler simulations with unstructured meshes, *J. Comput. Phys.* **84** (1989) 174–206.
[11] E. Godlewski and P.A. Raviart, *Hyperbolic Systems of Conservation Laws*, Math. Appl. (SMAI, Ellipses, Paris, 1991).
[12] D. Hänel, Effects of numerical dissipation in solutions of Navier–Stokes equations, Preprint, Aerodynamisches Institut, RWTH, Aachen, 1992.
[13] T. Hůlek, M. Huněk and K. Kozel, Numerical solution of Euler and Navier–Stokes equations for 2D transonic flow, in: Ch. Hirsch, J. Périaux and W. Kordula, Eds., *Computational Fluid Dynamics* **92**, *Vol. I, Proc. 1st European CFD Conf.* (Elsevier, Amsterdam, 1992) 61–68.
[14] P. Knobloch, Numerical modelling of viscous compressible flow, Master Degree Thesis, Faculty of Mathematics and Physics, Charles University, Prague, 1993 (in Czech).
[15] P.L. Lions, Global existence of solutions for isentropic compressible Navier–Stokes equations, *Math. Problems Mech.* **316** (I) (1993) 1335–1340.
[16] M. Lukáčová-Medvid'ová, Numerical solution of compressible flow, Ph.D. Thesis, Faculty of Mathematics and Physics, Charles University, Prague, 1994.
[17] S. Osher and F. Solomon, Upwind difference schemes for hyperbolic systems of conservation laws, *Math. Comp.* **38** (1982) 339–374.
[18] Th. Sonar, On the design of an upwind scheme for compressible flow on general triangulations, Preprint, DLR, Göttingen, 1993.
[19] Th. Sonar, J. Felcman, G. Warnecke and W. Wendland, Adaptive Berechnung kompressibler Strömungsfelder, in: *Strömungen mit Ablösung, Proc. 8th DGLR-Fach-Symp.* DGLR-Bericht 92-07, Bonn (1992) 345–350.
[20] S.P. Spekreijse, *Multigrid Solution of the Steady Euler Equations* (Center for Mathematics and Computer Science, Amsterdam, 1988).
[21] G. Vijayasundaram, Transonic flow simulation using upstream centered scheme of Godunov type in finite elements, *J. Comput. Phys.* **63** (1986) 416–433.
[22] R. Vilsmeier and D. Hänel, Adaptive solutions of the conservation equations on unstructured grids, in: J.B. Vos, A. Rizzi and J.L. Ryhming, Eds., *Proc. 9th GAMM Conf. on Numerical Methods in Fluid Mechanics*, Notes Numer. Fluid Mech. **35** (Vieweg, Braunschweig, 1992) 321–330.